

RESEARCH PAPER

Adsorption Study of Methylene Blue on to Powder Activated Carbon Prepared from Ananas comosus Peels

Nasiru Pindiga Yahaya^{1,2*}, Ibrahim Ali¹, Alhaji Madu Kolo³, Adamun Shehu¹

¹ Department of Chemistry, Faculty of Science, Bauchi State University, Gadau. P.M.B. 65, Gadau, Nigeria

² Department of Chemistry, Faculty of Science, Gombe State University, PMB 127 Gombe, Nigeria

³ Department of Chemistry, Faculty of Science, Abubakar Tafawa Balewa University, Bauchi. PMB 0248 Bauchi, Nigeria

ARTICLE INFO

Article History:

Received 16 Feb 2023

Accepted 29 Aug 2023

Published 01 Oct 2023

Keywords:

Activated Carbon,
Ananas Comosus Peels,
Plackett-Burman Design,
Methylene Blue.

ABSTRACT

The adsorption capacity of activated carbon powder prepared from Ananas comosus peels for the removal of methylene blue dye as a contaminant was investigated. These adsorbents were prepared by carbonization at 500 °C with activating agents (K₂CO₃, H₃PO₄ and NaOH) and characterized using Fourier Transform Infrared. Plackett-Burman Design was used to analyze the various factors affecting adsorption. Response surface methodology techniques was employed to determine the optimal condition of pH=12.6569 and adsorbent dosage of 1.1864. At the optimal condition, the activated carbon yielded the highest removal of methylene blue (99.4 %). The experimental data best fitted the pseudo-second order kinetic model, except for acid activation (ACP-A) which agreed with inter-particle diffusion model with the determination coefficient of 0.9939. The adsorption isotherms for all the prepared carbons were highly consistent with Langmuir adsorption isotherm. This study demonstrates that the activated carbon prepared from Ananas comosus peels can be efficient in removing methylene blue dye contaminants from aqueous solution.

How to cite this article

Ibrahim A., Pindiga Yahaya N., Madu Kolo A., Shehu A., Adsorption Study of Methylene Blue onto Powder Activated Carbon Prepared from Ananas comosus Peels. Nanochem. Res., 2023; 8(4): 231-242. DOI: 10.22036/NCR.2023.04.01

INTRODUCTION

Methylene blue as a heterocyclic aromatic compound, also known systematically as 3,7-bis(dimethylamino)-phenothiazin-5-ium chloride, is widely used in analytical chemistry for spectrophotometric determination of hydrogen sulfide [1] and as redox indicator [2-3]. It is also employed in medicine for the treatment of refractory hypertension, methemoglobinemia [4-6], sepsis in immunosuppressed patients [7] and as antidote for cyanide poisoning [8]. Despite its numerous medical and scientific applications, excessive consumption of methylene blue has been shown to have neurotoxic effects on the central nervous system [9]. Further, due to its widespread

use, a substantial quantity of methylene blue is released into aquatic environment during production, usage, and disposal, which can lead to an excess amount of methylene blue entering the food chain through bioaccumulation by aquatic biota. In addition to its harmful impact on human health, the contamination of aquatic environment by excess methylene blue (or any other dye) reduces the growth of algae by obstructing light required for photosynthesis, resulting in an ecological imbalance in the aquatic ecosystem [10]. One of the important processes for the removal of dyes from water is adsorption. Adsorption techniques have been demonstrated to be effective in removing colored organics. Adsorption is a process in which a substance

* Corresponding Author Email: np500@yahoo.com



This work is licensed under the Creative Commons Attribution 4.0 International License.

To view a copy of this license, visit <http://creativecommons.org/licenses/by/4.0/>.

is separated from a phase and accumulates or concentrates at the surface of another. It takes place when a liquid or most commonly a gas (the adsorbate) accumulates on the surface of a solid adsorbent, forming a molecular film. Activated carbon prepared from agricultural waste could serve as the best low-cost adsorbent used in this process. *Ananas comosus* peels activated carbon is particularly effective due to its high surface porosity. The textile and other chemical industries produce large amounts of highly colored waste products. To remove dyestuff from industrial wastewater, various processes can be employed, such as adsorption, oxidation-ozonation, biological processes, coagulation-flocculation, and membrane processes [11]. Adsorption is a process or method in which atoms, molecules, or ions are retained on the surfaces of solids through chemical or physical bonding. This process is a cost-effective way for removing dyes from wastewater. Among the processes mentioned above, adsorption has been identified as a key process for the reduction of dyestuff concentration in wastewater [12], and various adsorbents such as activated carbon, peat, chitin, and clay can be used to achieve this.

EXPERIMENTAL

Materials and Methods

Characterization is as important as developing the material; it is a judgmental analysis that verifies the material being developed or synthesized. Some conventional characterization techniques are discussed below.

The chemical functionality of peels (precursor) and its ACP(s) was quantitatively identified by Fourier transform infrared spectroscopy (FTIR). The FTIR spectra were recorded between 4000 and 400 cm^{-1} using an AVATAR 360 spectrophotometer (Thermo Nicolet Co., USA), and the transmission spectra of the samples were recorded using KBr pellets (0.1 % sample).

Scanning electron microscopy (SEM) was employed for identifying surface physical morphology. A JSM-6390LV (JEOL Ltd., Japan) instrument with a 3k accelerating voltage was used to characterize the morphology of ACP(s), which were dried overnight at approximately 105°C under vacuum prior to SEM analysis.

The apparatus, machines and the chemicals used in this research, along with their model manufacturers and purity, are presented in Tables

1 and 2. The apparatus used were washed with detergents, rinsed with distilled deionized water, and dried in an oven at 50°C for 2 hours.

Stock Solution of Methylene Blue

The stock solution of methylene blue (1000 mg/L) was prepared by dissolving 1 g of solid methylene blue in a 250 cm^3 beaker. The solution was then transferred into a 1000 cm^3 volumetric flask and diluted to the mark.

Stock Solution of Sodium Hydroxide

A 0.1M stock solution of sodium hydroxide (NaOH) was prepared by weighing 4 g of NaOH in a 250 cm^3 beaker and adding water. The resulting mixture was then transferred to 1000 cm^3 volumetric flask and diluted to the mark.

Stock Solution of Sodium Trioxonitrate

A 2M stock solution of sodium trioxonitrate (NaNO_3) was prepared by dissolving 170 g of NaNO_3 in a 250 cm^3 beaker containing water. The resulting mixture was then diluted to a total volume of 1000 cm^3 volumetric flask.

Stock of Nitric Acid

The stock of nitric acid (HNO_3) was prepared by measuring 6.34 cm^3 of concentrated nitric acid into a 250 cm^3 beaker containing water. The solution was transferred to 1dm³ volumetric flask and diluted with distilled water to the desired volume. The method described was adopted from [13-14].

Random selection techniques were applied for sample collection to prevent bias. Activated carbon was prepared from agricultural waste, functionalized, characterized and optimized, and then the sorption isotherm was tested.

Sample Collection and Preparation

Ananas comosus peels were obtained from Azare Central Market, Bauchi State Nigeria and taken to Botany Department Bauchi State University Gadau for identification. The peels were washed several times with distilled water, cut into smaller pieces, and air-dried [15]. The particles derived from *Ananas comosus* peels were then activated at 500°C for 2 hours, stored in air-tight container, and labeled ACP-T.

Preparation of Adsorbent (Activated Carbon) by Chemical Activation

Preparation of activated carbon (adsorbent) using

Table 1: List of machines/Apparatus used throughout this research

S/no	Name	Model	Manufacturer
i	Oven	DHG-9202	Gulex medical and scientific England
ii	Orbital Shaker	WSZ-100A	WSZ-series orbital shaker
iii	Uv-vis spectrophometer	UNICO UV-2100	UNICO Instrument Co., Ltd, Shanghai, China
iv	Weighing Balance	PA413	COHAUS coporation USA
v	Muffle furnace	TT-EF	Techmel and Techmel USA
vi	Crucibles	Ceramics	Gollenkamp, USA
vii	Stop watch	Digital	Ventus
viii	Funnel	Rubber	Pyrex England
ix	FTIR Spectrometer	VERTEX 70/70V	Agilent Technologies
x	SEM	800-07334	PHENOM SEM

Table 2: List of chemicals used throughout this research

S/no	Chemical	Purity (%)	Manufacturers
i	Methylene blue	97	Park Scientific limited Northampton, U.K
ii	Sodium hydroxide	97.5	Park Scientific limited Northampton, U.K
iii	Sodium nitrate	98	Park Scientific limited Northampton, U.K
iv	Nitric acid	69	Kermel
v	Phosphoric acid	85	Sigma-Aldrich

Potassium Trioxocarbonate (K_2CO_3) as activating agent

The solid waste (*Ananas comosus* peels) was washed with distilled water for removing impurities, and then oven-dried at 110 °C until a moisture content of 5-10 % was obtained. The sample was cut into small, random pieces. The method of activation used to prepare the activated carbon is described in [15]. The raw material (*Ananas comosus* peels) was added to a 500 mL beaker containing an activation agent (K_2CO_3) in a 1:1 ratio and left to immerse for 24 hours at 25 °C through occasional stirring with glass rod. The sample was then dried at 110 °C for 24 hours and carbonized at 500 °C for 1 hour before cooling to room temperature. The activated sample was washed by hot distilled water (30-50°C) to remove any unused activating agent, oven-dried at 110 °C for 24 hours, stored in a tightly sealed container, and labeled APC-S.

Preparation of activated carbon (adsorbent) using Phosphoric acid (H_3PO_4) as activating agent

Oven-dried *Ananas comosus* peels were soaked in a boiling solution of 40 % phosphoric acid (H_3PO_4) for 1 hour [16]. Subsequently, the *Ananas comosus* peels were oven-dried at 100 °C

for 24 hours [17] followed by being kept at room temperature for 24 hours [16]. The air-dried peels were then carbonized in a furnace at 500 °C for 1 hour [17]. Afterwards, the peels were washed with hot as well as cold deionized water and dried at 120 °C for 2 hours [18] before being stored in a tightly sealed container [16] and labeled APC-A.

Preparation of activated carbon (adsorbent) using sodium hydroxide (NaOH) as activating agent

Oven-dried *Ananas comosus* was stirred in a 4 % NaOH solution for 1 hour in a 1:20 ratio. It was then kept overnight [19] before being oven-dried at 300 °C for 3 hours. Subsequently, it was carbonized in a furnace at 200°C for 60 minutes and washed with a 0.5M hydrochloric acid (HCl) solution. The carbonized materials were then washed with hot deionized water until the pH reaches 5-8, followed by a rewashing with cool deionized water. The washed samples were dried in oven at 120 °C for 2 hours, stored in tight lid container [20], and labeled APC-B.

Optimization of Significant Factors

The effect of pH and the adsorbent dosage were investigated using response surface methodology

(RSM) techniques, employing central composite design. Here the various combinations of pH and adsorbent dosage were used. Run 1 used pH=3 and 0.1 g dosage; run 2 used pH=11 and adsorbent dosage of 0.1 g; run 3 used pH=3 and adsorbent dosage of 1.0 g; and run 4 used pH=11 and dosage of 1.0 g. Runs 5 pH level 1.35 adsorbent dose of 0.55, 6 pH 12.66 adsorbent dose of 0.55, 7 pH 7 adsorbent dose of 0.09, 8 pH 7 adsorbent dose 1.19, 9 pH 7 adsorbent dose 0.55, and 10 pH 7 adsorbent dose 0.55. The percentage of removal was measured for each run, and the highest percentage was selected as the optimal condition for pH and adsorbent dosage.

Investigation of Sorption Kinetics

An experiment was conducted for sorption kinetics by adding the selected dosage (1.1864 g) of ACP-T to six 250 cm³ Erlenmeyer flasks, each containing 50 cm³ of dye solution. The concentration of methylene blue in each flask throughout the study was kept fixed, while the optimal pH of 12.6569 was selected and the ionic strength of each solution was adjusted to 0.2. The flasks were then shaken at ambient temperature (28 °C) for specific periods of time (20, 40, 60, 80, 100, 120 minutes) using Orbital Shaker at high speed. The content of each flask was filtered and the residual concentrations of methylene blue in these filtrates were determined at a selected wavelength (λ_{\max} nm) using a UV-Vis spectrophotometer. The amount of methylene blue adsorbed onto the adsorbent at various time intervals were calculated using equation (3). This experiment was carried out twice and the fitness of the average data obtained was tested using the intraparticle diffusion model (equation 4), pseudo-first order model (equation 5) and pseudo-second order model (equation 6). The same procedure was repeated using ACP-S, ACP-A, and ACP-B.

$$q_t = \frac{V}{m}(C_i - C_t) \quad (3)$$

$$q_t = k_{int} t^{1/2} \quad (4)$$

$$\log(q_e - q_t) = \log q_e - \frac{k_1}{2.303} t \quad (5)$$

$$\frac{t}{q_t} = \frac{1}{k_2 q_e^2} + \frac{1}{q_e} t \quad (6)$$

Where q_t and q_e are the amount of adsorption at time t and equilibrium, respectively. In addition, k_1 and k_2 are the rate constants of the pseudo-first-order and pseudo-second-order adsorption processes, respectively.

Microsoft excel was used in plotting the scatter (Linear graphs), and the values obtained were compared with the equations (3, 4, 5 and 6) above.

Adsorption Isotherm

An experiment for isotherm was conducted by adding the selected dosage (1.1864 g) of ACP-T to six 250 cm³ Erlenmeyer flasks each containing 50 cm³ of 30 mg/L dye solution. The concentrations of methylene blue were adjusted to 60, 90, 120, 150, 180, and 210 mg/L for 7 flasks, respectively, and the optimal pH of 12.6569 was selected. The ionic strength of each solution was adjusted to 0.2. The flasks were then shaken at ambient temperature (28 °C) for 60 minutes using an orbital shaker at high speed. The filtrates of each flask were filtered and the residual concentrations of methylene blue in these filtrates were determined at a selected wavelength (λ_{\max} nm) using UV-Vis spectrophotometer. The amount of methylene blue adsorbed onto the adsorbent at various concentrations was calculated using equation (3). This experiment was carried out twice and the fitness of the average data obtained was evaluated using Langmuir Isotherm model (equation 7), and Freundlich Isotherm model (equation 8). The same procedure was repeated using ACP-S, ACP-A, and ACP-B.

$$\frac{C_e}{q_e} = \frac{1}{bq_{max}} + \frac{C_e}{q_{max}} \quad (7)$$

$$\ln q_e = \ln K_f + \frac{1}{n} \ln C_e \quad (8)$$

Where q_e is the concentration of methylene blue at equilibrium (mg/g); q_{\max} is the maximum methylene blue uptake per unit mass of activated carbon (mg/g) adsorption capacity; K is constant

Microsoft excel was used in plotting the scatter (linear graphs), and the values obtained were compared with the equations (7 and 8) above.

RESULTS AND DISCUSSION

The results are displayed in graphics and some in tabular form, and each result was discussed accordingly.

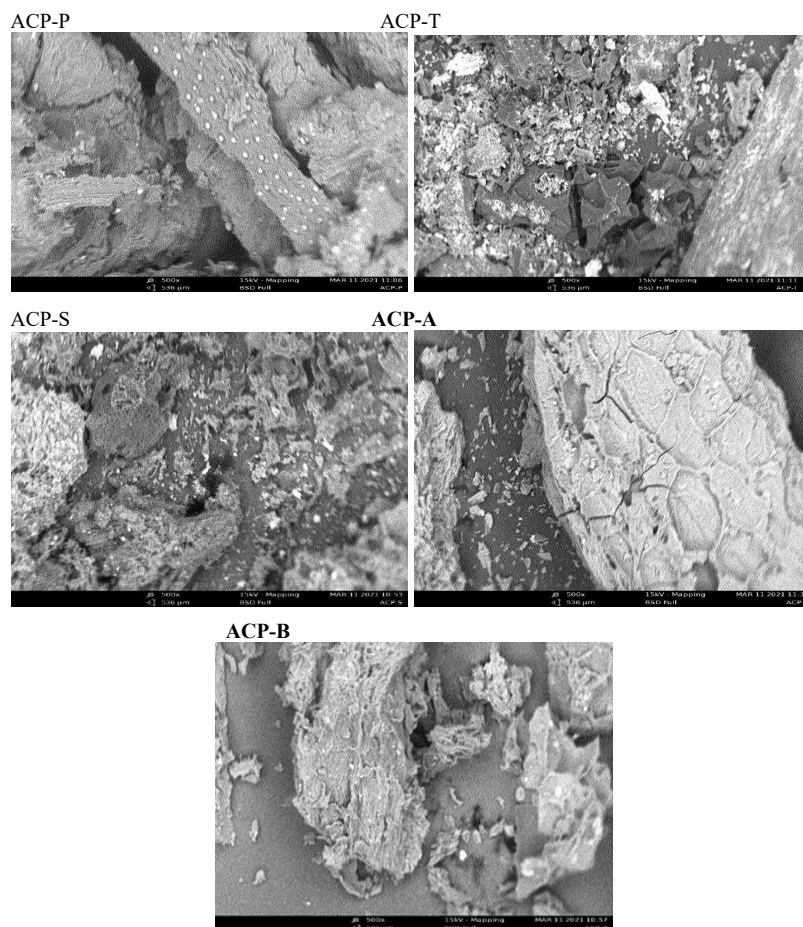


Fig. 1: The SEM image of precursor and activated ACP(s) before adsorption.

Morphology

The SEM images of the surface area of activated carbons revealed highly packed bundles of deep, long cylindrical pores and some pits (Fig. 1), suggesting a good adsorptive capacity [21]. The surface porosity of the activated carbons serves as the active sites for adsorption, thus increasing the surface area.

The results of Fig. 1 indicate that the APCs have a cubic morphology, with the presence of some larger particles that are monodispersed and partially spherical. The results obtained are in agreement with the literature reported by [22], which indicate a cubic morphology with the presence of some bigger particles attributed to the aggregation and overlapping of some smaller particles during the APCs preparation.

Fig. 1 displays the SEM images of all the ACP(s), showing that this inactivated material is nonporous. However, all activated *Ananas comosus* peels have porous structure. Additionally, comparing

the surface morphology of ACP-P with ACP-T, ACP-S, ACP-A and ACP-B, it is seen that ACP-B has much larger and deeper porous structure. This could explain the fast removal of methylene blue in this study, as these larger and deeper pores that are important factors for adsorption [22]. As a result, the base used to activate *Ananas comosus* peels appears to have a significant impact on the microstructure. In other words, the porosity of adsorbent might be adjusted using various bases, acids or salts.

Fourier Transform Infrared Spectroscopy

The following are the spectra of the prepared activated carbons, ACP(s).

The FT-IR spectra of precursor, thermal, salt, acid and base activation samples are shown in Figures 2-6. All sample spectra feature various distinct and sharp adsorption bands as well as relatively low intensity peaks.

The FT-IR studies of ACP-P presented in

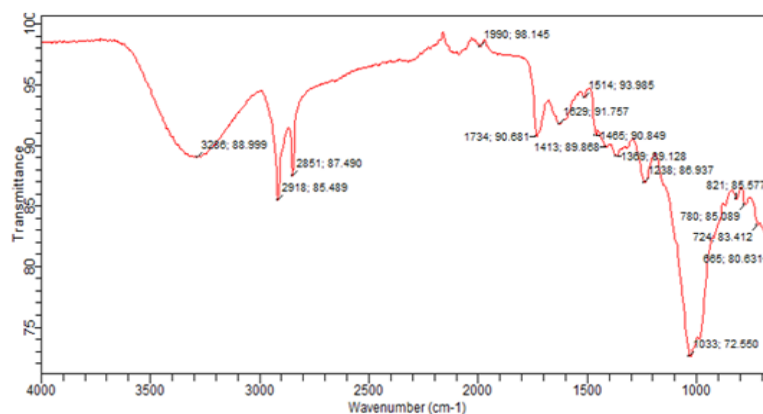


Fig. 2: FTIR of ACP-P

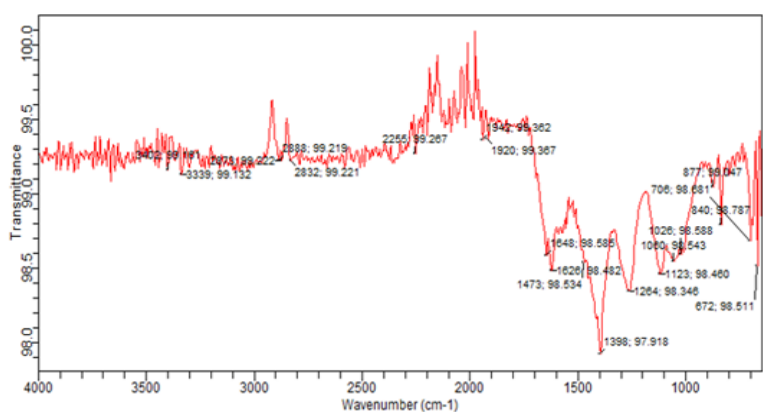


Fig. 3: FTIR of ACP-T

Fig. 2 reveal a sharp band at 2918 cm^{-1} , which is an asymmetric C-H stretching, and a peak at 2851 cm^{-1} , which is a symmetric C-H stretching of methylene (CH_2). The peak at 1734 cm^{-1} is aliphatic aldehyde C=O stretching while the peak at 1033 cm^{-1} is in-plane C-H bending. The band at 1514 cm^{-1} is attributed to C-C stretching in the aromatic ring, and the peak at 1413 cm^{-1} is related to C-C stretching in the ring. The broad band at 3286 cm^{-1} is ascribed to O-H stretching. The FT-IR spectra of the activated carbon ACP-A in Fig. 5 shows characteristic bands at 3141 cm^{-1} due to C-H stretching and at 3015.79 cm^{-1} which represent C-H stretching (aromatic) of the carboxylic acid. The peak at 2326 cm^{-1} represents the C-C stretching while that peak at 2113 cm^{-1} is related to $\text{C}\equiv\text{C}$ stretching. The peak at 1734 cm^{-1} is attributed to aliphatic aldehyde C=O stretching while the peak at 1441 cm^{-1} shows the C-H bond in CH_3 . The presence of C-O stretching was indicated by the peaks at 1138.04 cm^{-1} , 1099.46 cm^{-1} , and 1022.31 cm^{-1} . The peaks at 953 cm^{-1} and 742 cm^{-1} are

due to C-H deformation out-of-plane bending. The presence of these functional groups will increase the heterogeneity in adsorption. Fig. 6 shows that for ACP-B the band at 3674 cm^{-1} is due to O-H stretching and a trough at 3327 cm^{-1} for $-\text{C}\equiv\text{C}-\text{H}$; C-H stretching. The 2344 cm^{-1} band was attributed to the $\text{C}\equiv\text{C}$ stretching and the band at 1923 cm^{-1} is an overtone band. The peak at 2113 cm^{-1} is related to $-\text{C}\equiv\text{C}-$ stretching while the peak at 1562 cm^{-1} represents C=C stretch in the ring. The band at 1376 cm^{-1} is attributed to C-H methyl rock, 1316 cm^{-1} to methylene (CH_2) wagging, 760 cm^{-1} and 672 cm^{-1} to $\text{C}\equiv\text{C}-\text{H}$; C-H bending out of plane.

The peak at 3339 cm^{-1} in Fig. 3 regarding ACP-T is related to N-H stretching; the band at 2832 cm^{-1} indicates the presence of carboxylic acid, and the peak at 1626 cm^{-1} is ascribed to N-H bending primary. In addition, the peak at 1398 cm^{-1} is related to C-H aliphatic bending, and 1264 cm^{-1} to C-H wagging. The peak at 1123 cm^{-1} is attributed to C-O stretching band due to the C-O-C bond linkage in the compound, and the peak at 789 cm^{-1} is assigned to C-H out-of-plane. This corresponds

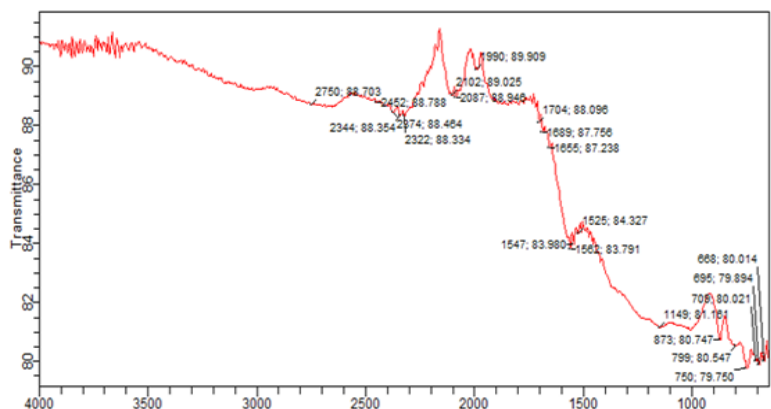


Fig. 4: FTIR of ACP-S

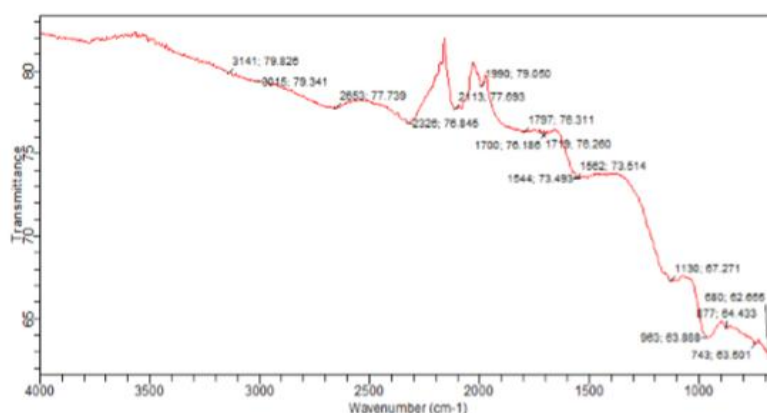


Fig. 5: FTIR of ACP-A

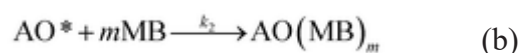
to the literature reported by [22]. The peak at 2760 cm^{-1} is indicative of aldehyde C-H stretching, while 2322 cm^{-1} corresponds to C-N stretching, 2087 cm^{-1} to $\text{C}\equiv\text{C}$ stretching, 1547 cm^{-1} to N-O asymmetric stretching, 799 cm^{-1} and 750 cm^{-1} to C-H out-of-plane bending (Fig. 4).

The adsorption mechanism: The adsorption rate of methylene blue (MB) is usually controlled by a one-step mechanism, which was determined by the reaction mechanism at low concentrations. However, at high MB concentrations, the adsorption process was more complex, requiring a multi-step reaction mechanism. The objective was to investigate the adsorption of the MB molecules on the CNS-based activated carbon.

The reaction of MB molecules and the vibrations of chemical functional groups were detected by the FT-IR analysis of the CNS-based activated carbons before and after adsorption tests.

Many-step reaction mechanism. The presence of the N-O bond 799 cm^{-1} (Fig. 4) on the adsorbent surface indicated that the adsorbed MB molecule

formed a chemical bond stretching with the active site, either directly or indirectly. The elementary reactions are detailed in Eqs (a) and (b):



Where AOH is an adsorbent surface including OH^- groups. The adsorption step is described by Eq. (b)

Optimization

Fig. 7 shows the optimal condition at which the maximum removal of the dye methylene blue dye occurs. For ACP-T, the pH of 12.6569 and adsorbent dosage of 1.1864g yields a 99.4 % removal of methylene blue dyes contaminant. Other factors were held constant throughout the research. For ACP-S, the pH is significant in the absence of adsorbent dosage. This may be due to the fact that potassium salt is higher in the activity series than sodium. Theoretically, potassium ion

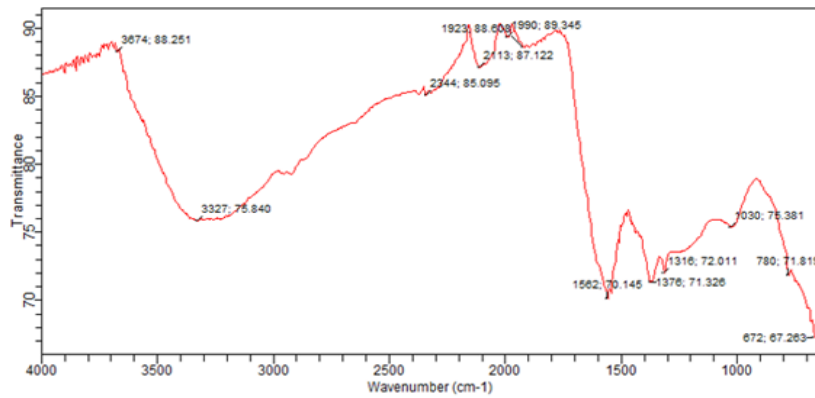


Fig. 6: FTIR of ACP-B

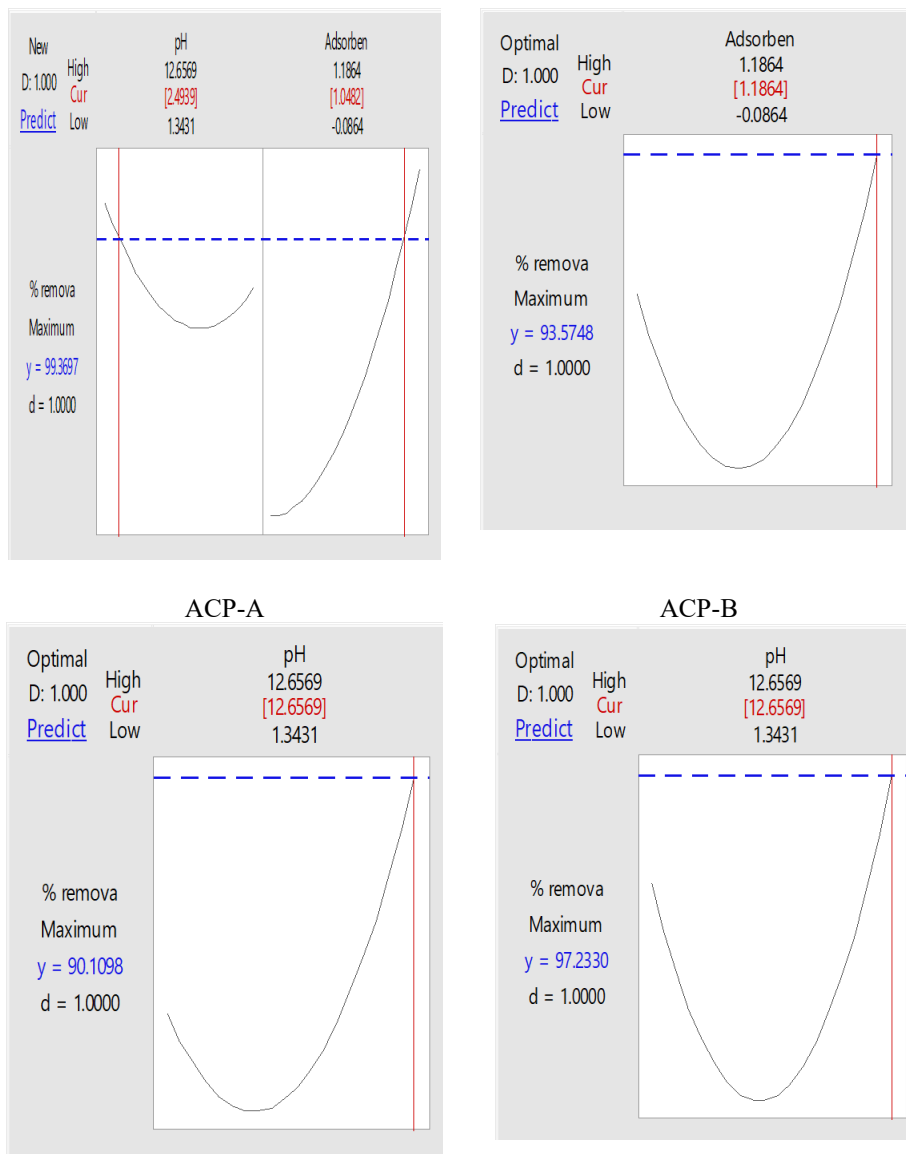


Fig. 7: Optimization of factors for ACP-T, ACP-S, ACP-A and ACP-B

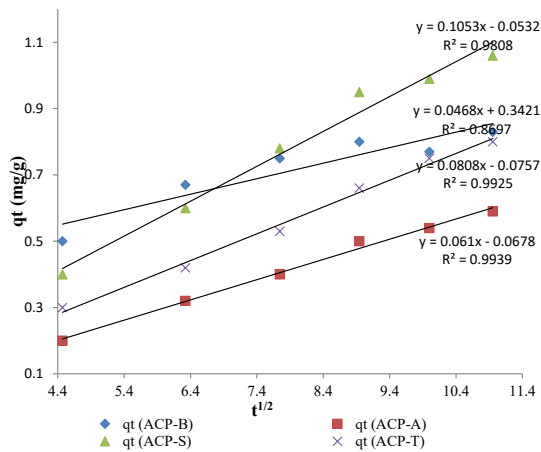


Fig. 8: Interparticle diffusion model for ACP-T, ACP-S, ACP-A and ACP-B

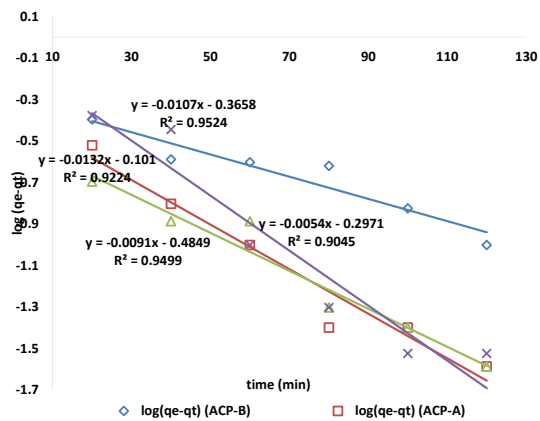


Fig. 9: Pseudo first order kinetics model for ACP-T, ACP-S, ACP-A and ACP-Ba

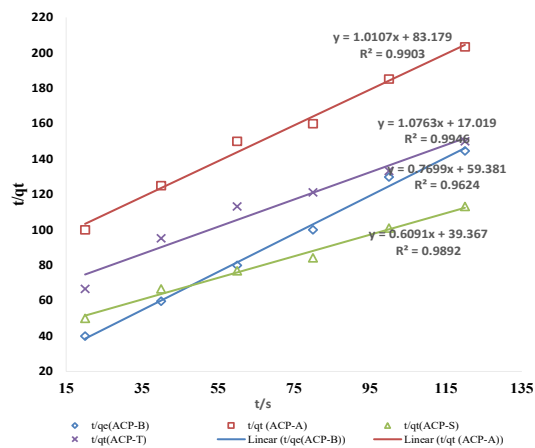


Fig. 10: Pseudo second order kinetics for ACP-T, ACP-S, ACP-A and ACP-B

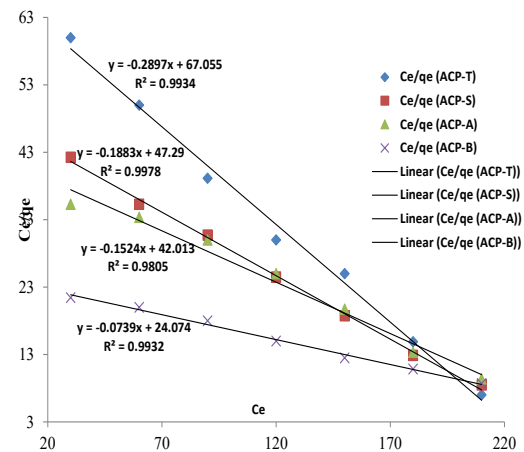


Fig. 11: Langmuir Adsorption Isotherm for ACP-T, ACP-S, ACP-A and ACP-B

should enhance the porosity of the surface of the materials (carbon) by increasing the surface area of the adsorbent. Fig. 7 also shows that in the presence of adsorbent dosage, pH does not appear in the regression. With fixed pH, ionic strength, and contact time, the highest removal of methylene blue dye contaminant (93.6 %) was recorded at an adsorbent dosage of 1.1864g.

For acid activation (ACP-A), a pH of 12.6569 was selected as the optimal condition, despite the adsorbent dosage being significant. The results indicates that pH and pH^* pH are more influential than the adsorbent dosage, thus making pH highly significant. This might be attributed to the influence of the acid during the activation of the adsorbent, at the mentioned optimal pH condition and the fixed values of other factors that are not significant.

ACP-A demonstrated a reasonable percentage removal of methylene blue dye (90.1 %).

Finally, the ACP-B was able to remove 97.2 % of methylene blue dye by adjusting the values of significant factors such as pH to 12.6569 and keeping the values of other insignificant factors constant.

Kinetic Studies

Figs. 8-10 display the plots interparticle diffusion model, pseudo first order model and pseudo second order model. The values of k_{int} , K_1 , and k_2 at room temperature were calculated from the slopes of the linear plots of $\log(q_e - q_t)$ versus t (min) (Fig. 9), t/q_e ($gm\ g^{-1}min$) versus t (min) (Fig. 10) and q_t (mg/g) versus $t^{1/2}$ ($min^{1/2}$) (Fig. 8). In addition, the kinetic parameters obtained for

Table 3. Kinetic models for ACP-T, ACP-S, ACP-A and ACP-B

Model	Kinetic Parameters	ACP-T	ACP-S	ACP-A	ACP-B
Pseudo first order	k_1 (min^{-1})	0.0304	0.0210	0.0246	0.0124
	q_e (mg/g)	0.7925	0.3274	0.4307	0.5045
	R^2	0.9224	0.9499	0.9524	0.9045
Pseudo second order	k_2 (g/mg.min)	0.0681	0.0094	0.0123	0.0100
	q_e (mg/g)	0.9291	1.6418	0.9894	1.2989
	R^2	0.9946	0.9892	0.9903	0.9624
Interparticle diffusion model	k_{int} (g/mg.min ^{1/2})	0.9925	0.1053	0.0610	0.0468
	R^2	0.9925	0.9808	0.9939	0.8697

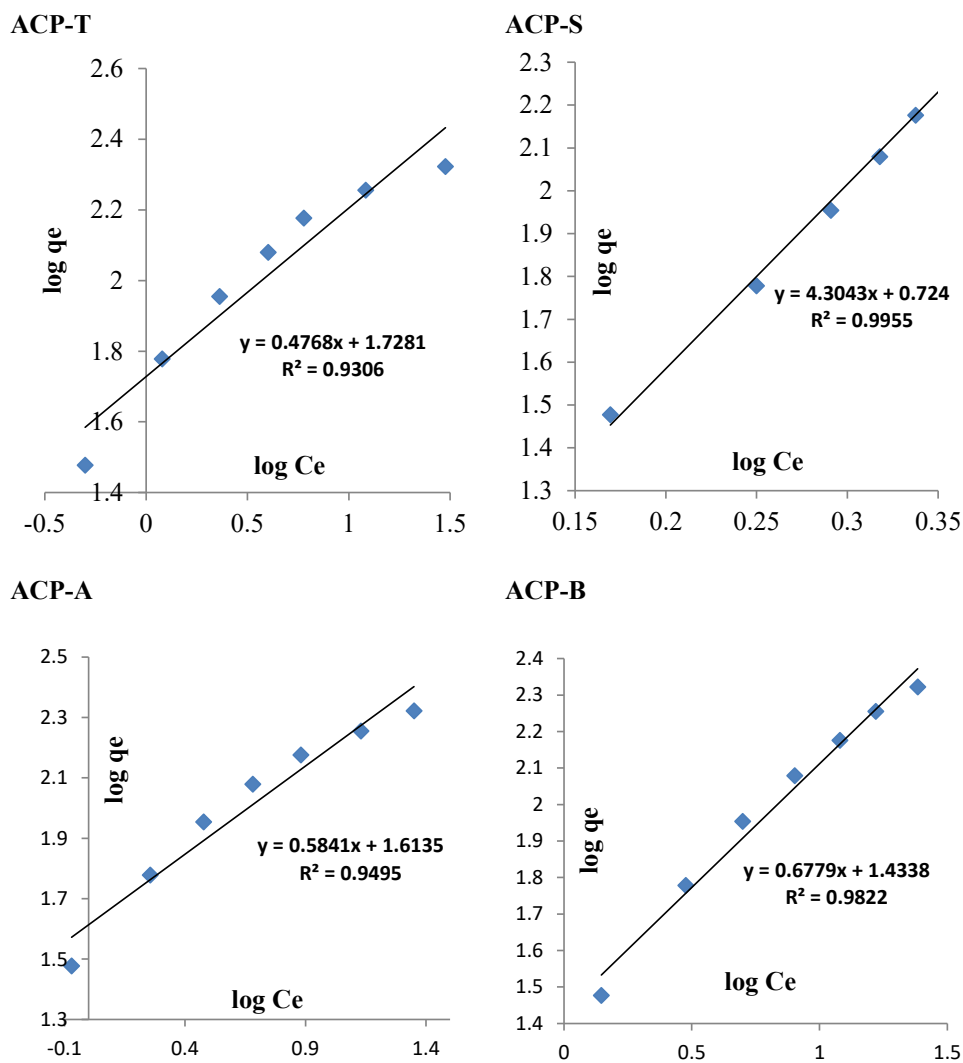


Fig. 12: Freundlich Adsorption Isotherm for ACP-T, ACP-S, ACP-A and ACP-B

Table 4. Isotherm Parameters

Isotherm Model	Parameters	ACP-T	ACP-S	ACP-A	ACP-B
Langmuir	q_{\max}	3.4518	5.3107	6.5617	13.5318
	B	0.0043	0.0040	0.0036	0.0031
	R^2	0.9934	0.9978	0.9805	0.9932
Freundlich	$1/n$	0.4768	4.3043	0.5841	0.6779
	K_f	53.4687	5.2966	41.0677	27.1519
	R^2	0.9306	0.9955	0.9495	0.9822

the adsorption of methylene blue onto activated carbon ACP-T, ACP-S, ACP-A and ACP-B were listed in Table 3. As can be seen from the table, the pseudo-second order kinetic model fitted well with a high correlation coefficient [17] and resulted in reasonable theoretical and experimental q_e values, with the exception of ACP-A.

The interparticle diffusion model with an R^2 value of 0.9939 was found to be a good fit for ACP-A, which could be due to the lower point of zero charge.

Adsorption Isotherm

Table 4. summarizes the adsorption parameters obtained from the plots displayed in Figs. 11 and 12 for Langmuir and Freundlich isotherms models, respectively. The data were best described by the Langmuir Isotherm, which had a high regression coefficient (R^2 value) for all the activated carbons prepared from Ananas comosus peels on methylene blue dye contaminant. The Langmuir adsorption isotherm is applicable only to monolayer adsorption, as the adsorbed molecules do not interact and all adsorption occurs through the same mechanism.

Tables 3 and 4 above present a summary of both kinetic models. The adsorption kinetics was determined under precise time conditions. The kind of adsorption process depends on the physiochemical characteristics of the adsorbent and system parameters such as temperature [23-24]. The linear graph of pseudo-first order was plotted from $\ln(q_e - qt)$ against t (mins) and the graph of pseudo-second order was plotted from t/qt against t (min). The results indicate that the pseudo-second order correlated better with the experimental data than the pseudo-first order. The pseudo-second order yielded much higher R^2 value than the pseudo-second order model, and

also the theoretical and experimental values are in good agreement with each other. Furthermore, the calculated q_e (cal) values are very close to q_e (exp) in the pseudo-second order model, and the R^2 values converge to 1, indicating the validity of the pseudo second order [25]. This demonstrates that the pseudo-second order is better fitted for the adsorption than that of pseudo-first order.

CONCLUSION

In this study, activated carbons were prepared from *Ananas comosus* peels, and the carbons had the desired porous with the point of zero charge acting as a buffer. Contact time and ionic strength were found to be insignificant, while pH and adsorbent dosage were significant, with 12.6569 and 1.1864g values, respectively. The highest removal percentage (99.4 %) of methylene blue from aqueous solution was recorded at the optimal condition of pH and adsorbent dosage. The experimental data best fitted the pseudo-second order kinetic model except for ACP-A, which agreed with interparticle diffusion model with the determination coefficient of 0.9939. The adsorption isotherms were highly consistent with the Langmuir isotherm. The activated carbons in this study found to be efficient in removing methylene blue dye contaminants, and could serve as an alternative (low cost) adsorbent for the removal of dyes (methylene blue) from wastewater.

CONFLICT OF INTEREST

The authors declare no conflicts of interest.

REFERENCES

1. Fogo JK, Popowsky M. Spectrophotometric Determination of Hydrogen Sulfide. *Analytical Chemistry*. 1949;21(6):732-4. <https://doi.org/10.1021/ac60030a028>
2. Prasetyo E, Mufakhir FR. Redox titration of iron using methylene blue as indicator and its application in ore analysis. *Asian Transactions on Basic Applied Sciences*

- 2011;1(5):1-9.
3. Weissgerber AJ. Methylene blue for refractory hypotension: a case report. AANA journal. 2008;76(4).
 4. Wendel WB. Use of Methylene Blue in Methemoglobinemia from Sulfanilamide Poisoning. Journal of the American Medical Association. 1937;109(15):1216. <https://doi.org/10.1001/jama.1937.02780410054018>
 5. Etteldorf JN. Methylene blue in the treatment of methemoglobinemia in premature infants caused by marking ink: A report of eight cases. The Journal of Pediatrics. 1951;38(1):24-7. [https://doi.org/10.1016/S0022-3476\(51\)80082-9](https://doi.org/10.1016/S0022-3476(51)80082-9)
 6. Paula B, Khurram J, Michael RK. Dapsone-induced methemoglobinemia. Canadian Family Physician. 2013;59(9):958.
 7. Ramamurthy V, Umamaheswari G, Nadu T, Nadu TJIJIRSET. Biodegradation of synthetic dyes by *Aspergillus terreus* inoculated on solid media. 2013;2(12):7821-7.
 8. Hanzlik PJ. Methylene Blue as Antidote for Cyanide Poisoning. Journal of the American Medical Association. 1933;100(5):357-. <https://doi.org/10.1001/jama.1933.02740050053028>
 9. Akinola L, Ibrahim A, Mohammed M. Adsorption of Methylene Blue on Adsorbents Derived From Delonix Regia Seed Pods and Vigna Subterranea Fruit Hulls: A Kinetic Study Adsorption of Methylene Blue on Adsorbent Derived from Delonix Regia Seed Pods and Vigna Subterranea Fruit Hulls: A Kinetic Study. Science World Journal. 2019;14:2019.
 10. Sousa M, Moraes P, Lopes P, Montagnolli R, Angelis D, Bidoia E. Contamination by Remazol Red Brilliant Dye and Its Impact in Aquatic Photosynthetic Microbiota. Environmental Management and Sustainable Development. 2012;1. <https://doi.org/10.5296/emsd.v1i2.2512>
 11. Santos SCR, Boaventura RAR. Adsorption modelling of textile dyes by sepiolite. Applied Clay Science. 2008;42(1):137-45. <https://doi.org/10.1016/j.clay.2008.01.002>
 12. McKay G, Porter JF, Prasad GR. The Removal of Dye Colours from Aqueous Solutions by Adsorption on Low-cost Materials. Water, Air, and Soil Pollution. 1999;114(3):423-38. <https://doi.org/10.1023/A:1005197308228>
 13. Baseri JR, Palanisamy PN, Sivakumar P. Comparative Studies of the Adsorption of Direct Dye on Activated Carbon and Conducting Polymer Composite. E-Journal of Chemistry. 2012;9:603196. <https://doi.org/10.1155/2012/603196>
 14. Akinola L. Adsorption of Crystal Violet onto Adsorbents Derived from Agricultural Wastes: Kinetic and Equilibrium Studies. Journal of Applied Sciences and Environmental Management. 2015;19:279-88. <https://doi.org/10.4314/jasem.v19i2.15>
 15. Rahman F, Akter M, Abedin M. Dyes removal from textile wastewater using orange peels. Int J Sci Technol Res. 2013;2:47-50.
 16. Banerjee K, Ramesh S, Gandhimathi R, P.V N. A Novel Agricultural Waste Adsorbent, Watermelon Shell For The Removal Of Copper From Aqueous Solutions. Iranica Journal Of Energy And Environment. 2012;3:143-56. <https://doi.org/10.5829/idosi.ijee.2012.03.02.0396>
 17. Geçgel Ü, Özcan G, Gürpınar GÇ. Removal of Methylene Blue from Aqueous Solution by Activated Carbon Prepared from Pea Shells (<i>Pisum sativum</i>). Journal of Chemistry. 2013;2013:614083. <https://doi.org/10.1155/2013/614083>
 18. Wang X, Li D, Li W, Peng J, Xia H, Zhang L, et al. Optimization of Mesoporous Activated Carbon from Coconut Shells by Chemical Activation with Phosphoric Acid. BioResources. 2013;8. <https://doi.org/10.15376/biores.8.4.6184-6195>
 19. Chin SX. Activated carbon's adsorbent by agricultural wastes in textile waste water: Faculty of Earth Sciences; 2014.
 20. Manickam Y. Characterization of durian husk as activated carbon: Faculty of Agro-Based Industry; 2014.
 21. Ashtaputrey S, Ashtaputrey P. Preparation, characterization and application of pineapple peel activated carbon as an adsorbent for water hardness removal. Journal of Chemical Pharmaceutical Research 2016;8(8):1030-4.
 22. Delibas A. Removal of Methylene Blue Using Fast Sucking Adsorbent. Journal of materials and Environmental Sciences. 2017;8:398-409.
 23. Yahaya N, Walid A, Abdullahi A, Mohammad A. Kinetic, Equilibrium and Thermodynamic Study of the Adsorption of Pb (II) and Cd (II) Ions from Aqueous Solution by the Leaves Biomass of Guava and Cashew Plants. Online Journal of Chemistry. 2022;2:23-38. <https://doi.org/10.31586/ojc.2022.263>
 24. Pindiga NY, Abubakar A, Danbature WL, Yakubu U. Green Synthesis and Characterization of Iron Nanoparticles from the Leaf Extract of *Khaya senegalensis* (Mahogany) and its Antimicrobial Activity. 2022. <https://doi.org/10.31586/ojc.2022.158>
 25. Yahaya N, Deedat A, Madugu Y, Abubakar Adamu A. Kinetic, Equilibrium and Thermodynamics Study of the Adsorption of Pb(II), Cu(II) and Ni(II) from Aqueous Solution using *Mangifera indica* Leaves. Trends Journal of Sciences Research. 2022;1:16-29. <https://doi.org/10.31586/materials.2022.262>